

# Experimental Liquidus Studies of the Pb-Fe-Ca-O System in Air

M. Shevchenko<sup>1</sup> · E. Jak<sup>1</sup>

Submitted: 26 October 2018 / in revised form: 24 November 2018 / Published online: 2 January 2019  
© ASM International 2019

**Abstract** Phase equilibria of the Pb-Fe-Ca-O system have been investigated at 1043–1653 K (770–1380 °C) for oxide liquid in equilibrium with air and solid oxide phases: (a) hematite  $\text{Fe}_2\text{O}_3$ ; (b) spinel  $(\text{Fe,Ca})\text{Fe}_2\text{O}_4$ ; (c) calcium ferrites  $\text{CaFe}_4\text{O}_7$ ,  $\text{CaFe}_2\text{O}_4$ ,  $\text{Ca}_2\text{Fe}_2\text{O}_5$ ; (d) lead ferrites (magnetoplumbite  $(\text{Pb,Ca})\text{O} \cdot 12\text{FeO}_{1.5}$ , plumboferrite  $(\text{Pb,Ca})\text{O} \cdot (5 + x)\text{FeO}_{1.5}$ , 1:1 lead ferrite  $(\text{Pb,Ca})\text{O} \cdot (1 \pm x)\text{FeO}_{1.5}$ ); (e) lead oxide PbO (massicot); (f) calcium plumbate  $\text{Ca}_2\text{PbO}_4$ ; and (g) lime CaO. High-temperature equilibration on inert metal (platinum, gold) substrates, followed by quenching and direct measurement of Pb, Fe and Ca concentrations in the phases with the electron probe x-ray microanalysis (EPMA) has been used to accurately characterize the system in equilibrium with air. All results are projected onto the PbO–“ $\text{FeO}_{1.5}$ ”–CaO plane for presentation purposes. The present study is the first systematic characterization of liquidus over a wide range of compositions in this system in equilibrium with air.

**Keywords** iron · lead · lime · phase diagrams · slags

## 1 Introduction

The chemical compositions of slags in typical lead smelting operations can be represented by the Pb-Zn-Fe-Cu-Ca-Si-Al-Mg-O system. Accurate data on slag-solid-metal phase equilibria, activities of lead species in the slag, and partitioning of elements between gas, slag, metal and solid

phases are essential to support further improvement of existing and development of new complex lead smelting, refining and recycling processes.

The present experimental study of the gas-slag-solid oxide phase equilibria in the Pb-Fe-Ca-O “low-order” system is an important part of an integrated thermodynamic modeling and experimental research program for the above multicomponent system. The earlier studies of the lead-containing slag systems<sup>[1–11]</sup> were focused on the multicomponent Pb-Zn-Fe-Ca-Si-O equilibria in air. Only one attempt to investigate the silica-free part of that system in reducing conditions was found in literature—the PbO concentration in the Pb-Fe-Ca-O slags in equilibrium with solid Fe and liquid Pb metals has been studied by Kudo et al.<sup>[12]</sup>; however, those results correspond to the significantly more reducing conditions in the PbO–“FeO”–CaO system with negligible ferric iron and low PbO concentrations.

According to the current public FactSage 6.2 thermodynamic database,<sup>[13–16]</sup> the liquidus surface in the PbO–“ $\text{FeO}_{1.5}$ ”–CaO system in equilibrium with air contains the hematite  $\text{Fe}_2\text{O}_3$ , spinel  $\text{Fe}_3\text{O}_{4+x}$ , magnetoplumbite “ $\text{PbFe}_{10}\text{O}_{16}$ ”, plumboferrite “ $\text{PbFe}_4\text{O}_7$ ”, lead ferrite  $\text{Pb}_2\text{Fe}_2\text{O}_5$ , massicot PbO, calcium plumbate  $\text{Ca}_2\text{PbO}_4$ , lime CaO, calcium ferrites  $\text{Ca}_2\text{Fe}_2\text{O}_5$ ,  $\text{CaFe}_2\text{O}_4$ , and  $\text{CaFe}_4\text{O}_7$  primary phase fields. No experimental studies reporting the extents of these phase fields in the PbO-FeO- $\text{Fe}_2\text{O}_3$ -SiO<sub>2</sub> system were found in literature. The current study focuses on the equilibria of the slag-(solid oxide)-air phases over wide range of temperatures [1043–1653 K (770–1380 °C)] and compositions.

✉ M. Shevchenko  
m.shevchenko@uq.edu.au

<sup>1</sup> Pyrometallurgy Innovation Centre (PYROSEARCH), The University of Queensland, Brisbane, QLD 4072, Australia

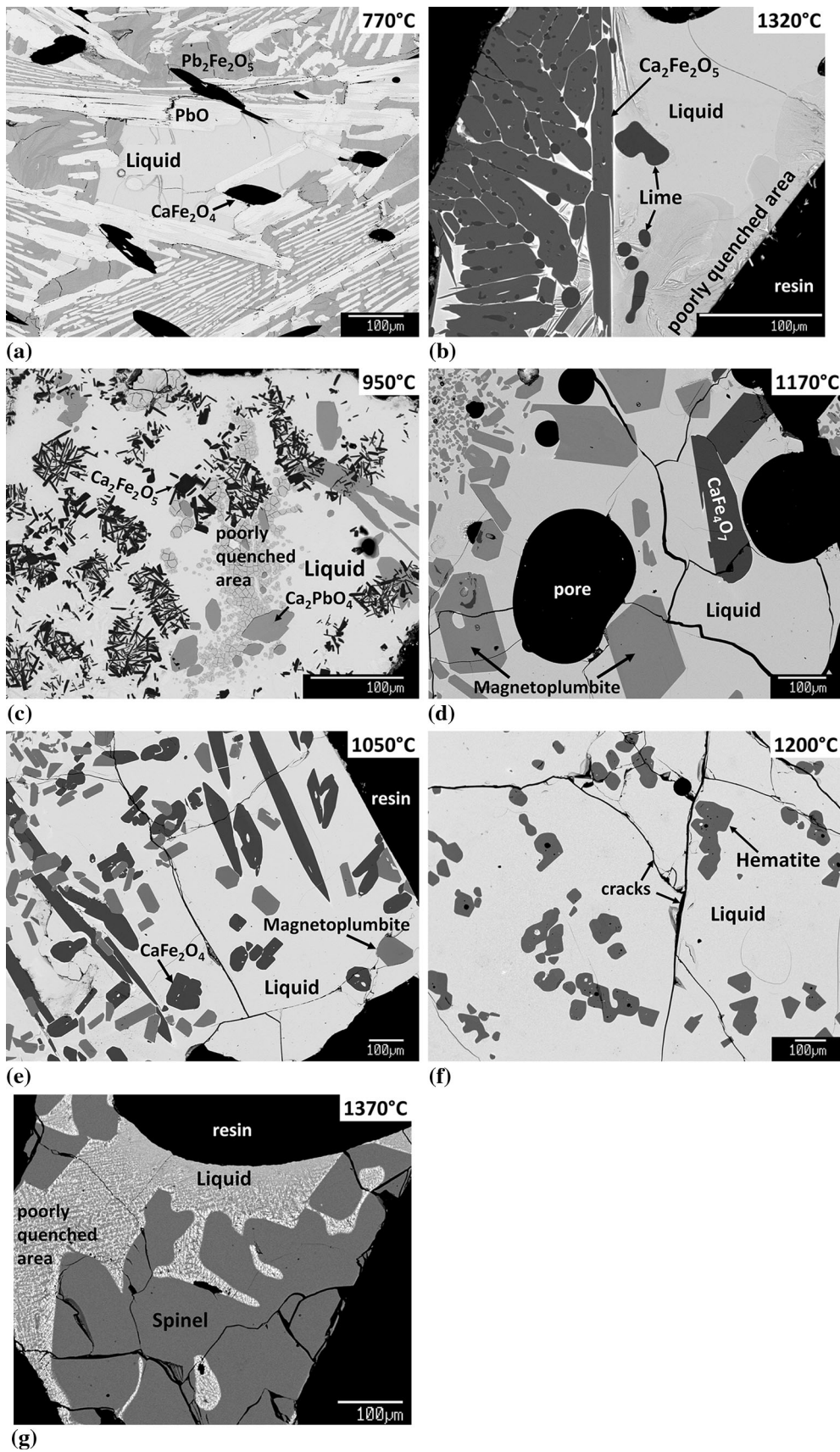


**Fig. 1** Backscattered scanning electron micrographs of quenched slag in the PbO–“FeO<sub>1.5</sub>”–CaO system in equilibrium with one or two crystalline phases and air,  $p(\text{O}_2) = 0.21$  atm. (a) Liquid + 1:1 lead ferrite  $\text{Pb}_2\text{Fe}_2\text{O}_5$  + massicot  $\text{PbO} + \text{CaFe}_2\text{O}_4$ . (b) Liquid + lime  $\text{CaO} + \text{Ca}_2\text{Fe}_2\text{O}_5$ . (c) Liquid +  $\text{Ca}_2\text{PbO}_4 + \text{Ca}_2\text{Fe}_2\text{O}_5$ . (d) Liquid + magnetoplumbite  $(\text{Pb,Ca})\text{Fe}_{12}\text{O}_{19} + \text{CaFe}_4\text{O}_7$ . (e) Liquid + magnetoplumbite  $(\text{Pb,Ca})\text{Fe}_{12}\text{O}_{19} + \text{CaFe}_2\text{O}_4$ . (f) Liquid + hematite  $\text{Fe}_2\text{O}_3$ . (g) Liquid + spinel  $(\text{Fe,Ca})\text{Fe}_2\text{O}_4$ . \*Liquid in (a) may be metastable and remaining due to local deviation of temperature or  $p(\text{O}_2)$ , or minor impurity ( $< 0.1$  mol.%)

## 2 Experimental Technique and Procedure

### 2.1 Experimental Procedure and Sample Examination

The experimental procedure and apparatus have been described in detail in previous publications by the authors at The Pyrometallurgy Innovation Centre, The University of Queensland.<sup>[11, 17]</sup> Initial mixtures were made from high-purity powders of  $\text{Fe}_2\text{O}_3$  (99.945 wt.% purity),  $\text{PbO}$  (99.9 wt.% purity),  $\text{CaCO}_3$  (99.9–99.99 wt.% purity), supplied by Alfa Aesar, MA, USA. The initial compositions of the mixtures were selected so that following the experiments one or more crystalline phases would be present in equilibrium with liquid slag. The volume fraction of solids in the final phase assemblage in the range of relatively fluid liquid was targeted to be below 50%, and preferably about 10%, to achieve acceptable quenching (to avoid crystallization during quenching). An iterative procedure involving preliminary experiments was often needed to achieve the targeted proportion of the phases for given final temperature and composition, since the exact liquidus coordinates were not initially known. Less than 0.5 g of mixture was used in each equilibration experiment.

Two types of substrates were used for equilibration, depending on the conditions:

1. Platinum foil envelopes ( $> 99.9\%$  purity, 0.05 mm thickness, provided by Johnson Matthey, Australia) were used for the equilibration of samples at temperatures above 1173–1273 K (900–1000 °C). At lower temperatures, a significant solubility of Pt in  $\text{CaFe}_2\text{O}_4$  compound was observed. Other platinum-based compounds, such as  $\text{PbPt}_2\text{O}_4$  and  $\text{Pb}_2\text{PtO}_4$ ,<sup>[18]</sup>  $\text{Ca}_4\text{PtO}_6$  and  $\text{CaPtO}_3$ <sup>[19]</sup> can form at low temperatures.
2. Gold foil baskets (99.99% purity, 0.127 mm thickness, provided by Sigma Aldrich, Australia) were used for the equilibration of  $\text{PbO}$ -rich slags with various primary solid phases at or below 1223 K (950 °C).

All equilibration experiments were carried out in a vertical reaction tube (impervious recrystallized alumina,

30-mm inner diameter) within an electrical resistance heated silicon carbide (SiC) furnace, bottom open to ensure natural air flow. A working thermocouple in a recrystallized alumina sheath was placed immediately next to the sample to monitor the actual sample temperature. The working thermocouple was periodically calibrated against a standard thermocouple (supplied by the National Measurement Institute of Australia, NSW, Australia). The overall absolute temperature accuracy of the experiments was estimated to be  $\pm 3$  K.

The sample was suspended in the hot zone of the furnace by Kanthal wire (0.7 or 1-mm diameter). Samples were pre-melted for various times at 20–130 K above the final equilibration temperature, to form a homogeneous slag. This was followed by equilibration at the final target temperature for the required time (0.25–18 h, see Table 2), to allow solid phases to crystallize from the melts. For experiments at high temperatures,  $> 1573$  K (1300 °C), samples were not pre-melted, to reduce the evaporation of  $\text{PbO}$ . At the end of the equilibration process, the sample was rapidly quenched in iced  $\text{CaCl}_2$  or  $\text{NaCl}$  brine [ $< 253$  K ( $-20$  °C)]. The specimen was then washed thoroughly in water and ethanol before being dried on a hot plate, and mounted in epoxy resin. Cross-sections were then prepared using conventional metallographic polishing techniques. Samples containing the lime ( $\text{CaO}$ ) phase were polished in kerosene to strictly limit contact with water.

The samples were examined by optical microscopy, carbon-coated, and the phase compositions were measured using an electron probe x-ray microanalysis technique with wavelength dispersive detectors (JEOL 8200L EPMA; Japan Electron Optics Ltd., Tokyo, Japan). EPMA was operated with 15-kV accelerating voltage and 20 nA probe current using the Duncumb–Philibert atomic number, absorption, and fluorescence correction (ZAF correction). Hematite ( $\text{Fe}_2\text{O}_3$ ), wollastonite ( $\text{CaSiO}_3$ ) (supplied by Charles M. Taylor Co., Stanford, CA, USA), and K-456 lead silicate glass (71 wt. pct.  $\text{PbO}$ , supplied by NIST, Washington, DC, USA) standards were used for calibration of EPMA. In addition, calcium ferrites  $\text{CaFe}_4\text{O}_7$ ,  $\text{CaFe}_2\text{O}_4$  and  $\text{Ca}_2\text{Fe}_2\text{O}_5$ , lime  $\text{CaO}$ , and calcium plumbate  $\text{Ca}_2\text{PbO}_4$ <sup>[20]</sup> were synthesized, and taken as secondary standards for EPMA with assumption of their stoichiometric composition. The measured compositions of these secondary standards systematically differed from the stoichiometric ratios by 0.4–0.5 mol.% towards excess of  $\text{CaO}$ . Subsequent additional correction was developed and applied to the values after the JEOL ZAF correction:

$$x(\text{PbO})^{\text{corr}} = x(\text{PbO}) + 0.0192 \cdot x(\text{PbO}) \cdot x(\text{CaO}) \quad (\text{Eq 1})$$

**Table 1** Experimental compositions of phases in the PbO–FeO<sub>1.5</sub>–CaO system in air

Substrate	Premelt T, °C	Final T, °C	Time, h*	Phase	Corrected mol.%						
					PbO	FeO <sub>1.5</sub>	CaO				
1:1 lead ferrite (Pb,Ca)FeO <sub>2.5</sub> + calcium ferrite CaFe <sub>2</sub> O <sub>4</sub> + massicot PbO eutectic											
Au foil	900	770	0.5 + 18	Liquid	74.9	22.6	2.5				
				CaFe <sub>2</sub> O <sub>4</sub>	0.40	66.5	33.1				
				1:1 lead ferrite	51.3	45.8	2.9				
				Massicot	99.71	0.11	0.18				
1:1 lead ferrite (Pb,Ca)FeO <sub>2.5</sub> + calcium ferrite CaFe <sub>2</sub> O <sub>4</sub> boundary											
Au foil	930	800	0.25 + 18	Liquid	71.4	26.0	2.6				
				CaFe <sub>2</sub> O <sub>4</sub>	0.27	66.6	33.2				
				1:1 lead ferrite	46.2	50.9	2.9				
Plumboferrite (Pb,Ca)Fe <sub>5</sub> O <sub>8.5</sub> + calcium ferrite CaFe <sub>2</sub> O <sub>4</sub> boundary											
Au foil	930	850	0.25 + 18	Liquid	63.1	33.9	2.9				
				Plumboferrite	14.8	82.9	2.2				
				CaFe <sub>2</sub> O <sub>4</sub>	0.11	66.6	33.3				
				Pt foil	930	900	0.25 + 18	Liquid	57.6	38.4	4.0
								Plumboferrite	14.8	82.8	2.3
								CaFe <sub>2</sub> O <sub>4</sub>	0.09	66.5	33.4
Magnetoplumbite (Pb,Ca)Fe <sub>10</sub> O <sub>16</sub> + calcium ferrite CaFe <sub>2</sub> O <sub>4</sub> boundary											
Pt foil	1050	950	0.25 + 2.5	Liquid	51.6	43.0	5.4				
				Magnetoplumbite	9.2	89.2	1.6				
				CaFe <sub>2</sub> O <sub>4</sub>	0.09	66.6	33.3				
Pt foil	1050	1000	0.25 + 2.5	Liquid	45.3	47.6	7.1				
				Magnetoplumbite	9.2	88.6	2.2				
				CaFe <sub>2</sub> O <sub>4</sub>	0.08	66.7	33.2				
Pt foil	1150	1050	0.25 + 2	Liquid	37.4	52.6	10.0				
				Magnetoplumbite	6.9	90.6	2.5				
				CaFe <sub>2</sub> O <sub>4</sub>	0.06	66.8	33.2				
Pt foil	1150	1100	0.25 + 2	Liquid	27.1	58.7	14.2				
				Magnetoplumbite	7.0	90.5	2.5				
				CaFe <sub>2</sub> O <sub>4</sub>	0.06	67.0	33.0				
Pt foil	1170	1150	0.25 + 1.5	Liquid	15.7	64.4	19.9				
				Magnetoplumbite	5.5	91.1	3.4				
				CaFe <sub>2</sub> O <sub>4</sub>	0.03	66.6	33.3				
Calcium ferrite CaFe <sub>2</sub> O <sub>4</sub> liquidus											
Pt foil	1170	1150	0.25 + 1.5	Liquid	18.9	60.3	20.8				
				CaFe <sub>2</sub> O <sub>4</sub>	0.03	66.6	33.3				
Magnetoplumbite (Pb,Ca)Fe <sub>10</sub> O <sub>16</sub> + calcium diferrite CaFe <sub>4</sub> O <sub>7</sub> boundary											
Pt foil	1250	1170	0.25 + 2	Liquid	9.4	67.8	22.8				
				Magnetoplumbite	4.1	91.7	4.2				
				CaFe <sub>4</sub> O <sub>7</sub>	0.43	79.7	19.9				
Hematite Fe <sub>2</sub> O <sub>3</sub> liquidus											
Pt foil	1230	1200	0.2 + 1.5	Liquid	7.3	71.6	21.1				
				Hematite	0.02	99.98	0.00				
Pt foil	1230	1200	0.2 + 1.5	Liquid	6.6	71.8	21.6				
				Hematite	0.02	99.98	0.00				
Pt foil	1230	1200	0.2 + 1.5	Liquid	5.3	72.3	22.4				
				Hematite	0.02	99.98	0.00				

**Table 1** continued

Substrate	Premelt T, °C	Final T, °C	Time, h*	Phase	Corrected mol.%		
					PbO	FeO <sub>1.5</sub>	CaO
Pt foil	1230	1200	0.2 + 1.5	Liquid	3.3	72.5	24.2
				Hematite	0.02	99.98	0.00
Pt foil	1250	1220	0.2 + 1.5	Liquid	8.2	71.0	20.8
				Hematite	0.03	99.97	0.00
Pt foil	1250	1220	0.2 + 1.5	Liquid	7.8	71.1	21.1
				Hematite	0.03	99.97	0.00
Pt foil	1280	1250	0.25 + 1.5	Liquid	6.9	72.5	20.6
				Hematite	0.00	100.00	0.00
Pt foil	No	1370	0.3	Liquid	7.5	80.8	11.7
				Hematite	0.00	100.00	0.00
Pt foil	No	1380	0.3	Liquid	13.0	80.0	7.0
				Hematite	0.02	99.98	0.00
Spinel (Fe,Ca)Fe <sub>2</sub> O <sub>4</sub> liquidus							
Pt foil	No	1370	0.3	Liquid	2.7	81.5	15.9
				Spinel	0.04	97.3	2.6
Pt foil	No	1370	0.3	Liquid	3.6	81.3	15.1
				Spinel	0.07	97.5	2.5
Pt foil	No	1370	0.3	Liquid	5.4	81.1	13.5
				Spinel	0.06	97.7	2.2
Dicalcium ferrite Ca <sub>2</sub> Fe <sub>2</sub> O <sub>5</sub> + calcium ferrite CaFe <sub>2</sub> O <sub>4</sub> boundary							
Au foil	1000	900	0.25 + 3	Liquid	64.4	30.1	5.5
				Ca <sub>2</sub> Fe <sub>2</sub> O <sub>5</sub>	1.3	49.7	49.0
				CaFe <sub>2</sub> O <sub>4</sub>	0.14	66.6	33.3
Dicalcium ferrite (brownmillerite) Ca <sub>2</sub> Fe <sub>2</sub> O <sub>5</sub> liquidus							
Au foil	1020	1000	0.2 + 1	Liquid	57.9	33.6	8.5
				Ca <sub>2</sub> Fe <sub>2</sub> O <sub>5</sub>	1.2	49.8	49.0
Pt foil	1200	1100	0.25 + 2	Liquid	34.9	50.7	14.4
				Ca <sub>2</sub> Fe <sub>2</sub> O <sub>5</sub>	0.74	50.0	49.2
Pt foil	1250	1200	0.25 + 1	Liquid	23.3	53.8	23.0
				Ca <sub>2</sub> Fe <sub>2</sub> O <sub>5</sub>	0.65	50.0	49.3
Dicalcium ferrite Ca <sub>2</sub> Fe <sub>2</sub> O <sub>5</sub> + calcium plumbite Ca <sub>2</sub> PbO <sub>4</sub> boundary							
Au foil	1020	950	0.2 + 2	Liquid	79.4	7.3	13.3
				Ca <sub>2</sub> Fe <sub>2</sub> O <sub>5</sub>	0.84	49.7	49.5
				Ca <sub>2</sub> PbO <sub>4</sub>	32.4	0.9	66.7
Dicalcium ferrite Ca <sub>2</sub> Fe <sub>2</sub> O <sub>5</sub> + lime CaO boundary							
Au foil	1020	1000	0.2 + 1	Liquid	75.2	8.5	16.3
				Ca <sub>2</sub> Fe <sub>2</sub> O <sub>5</sub>	0.28	49.9	49.8
				Lime	0.56	0.04	99.40
Pt foil	1120	1100	0.1 + 1	Liquid	67.9	12.4	19.7
				Ca <sub>2</sub> Fe <sub>2</sub> O <sub>5</sub>	1.4	49.7	48.9
				Lime	0.56	0.05	99.40
Pt foil	No	1320	0.2	Liquid	23.8	35.3	40.9
				Ca <sub>2</sub> Fe <sub>2</sub> O <sub>5</sub>	0.35	49.8	49.9
				Lime	0.51	0.21	99.28
Lime CaO liquidus							
Pt foil	No	1300	0.25	Liquid	28.9	33.7	37.4
				Lime	0.52	0.19	99.29

**Table 1** continued

Substrate	Premelt T, °C	Final T, °C	Time, h*	Phase	Corrected mol.%		
					PbO	FeO <sub>1.5</sub>	CaO
Pt foil	No	1320	0.2	Liquid	27.1	34.0	38.9
				Lime	0.51	0.21	99.28

Italics values are those below the estimated uncertainty level (0.1 mol.%)

\*Times are listed as (premelt time) + (equilibration time) or (premelt time) + (precrySTALLIZATION time) + (equilibration time)

**Table 2** Composition ranges of solid primary phases at the PbO–FeO<sub>1.5</sub>–CaO liquidus in air

Phase name	Formula	No. of points	Composition range, mol.%
Hematite	Fe <sub>2</sub> O <sub>3</sub>	9	< 0.01% CaO*, < 0.03% PbO*
Spinel	(Fe,Ca)Fe <sub>2</sub> O <sub>4+x</sub>	3	< 2.6% CaO, < 0.07% PbO*
Brownmillerite, dicalcium ferrite	(Ca <sub>1-x</sub> Pb <sub>x</sub> )O·FeO <sub>2.5</sub> , 0 < x < 0.027	8	< 1.4% PbO
Harmunite, monocalcium ferrite	CaFe <sub>2</sub> O <sub>4</sub>	11	< 0.40% PbO
Grandiferrite, calcium diferrite	CaFe <sub>4</sub> O <sub>7</sub>	1	< 0.43% PbO
Magnetoplumbite	(Pb <sub>1-x</sub> Ca <sub>x</sub> )O·(12 - y)FeO <sub>1.5</sub> , 0 < x < 0.5, 0 < y < 2	6	< 4.2% CaO
Plumboferrite	(Pb <sub>1-x</sub> Ca <sub>x</sub> )O·5FeO <sub>1.5</sub> , 0 < x < 0.14	2	< 2.3% CaO
1:1 lead ferrite	(Pb <sub>1-x</sub> Ca <sub>x</sub> )O·yFeO <sub>1.5</sub> , 0 < x < 0.06, 0.9 < y < 1.1	2	< 2.9% CaO
Calcium plumbate	Ca <sub>2</sub> PbO <sub>4</sub>	1	< 0.9% FeO <sub>1.5</sub>
Lime	CaO	5	< 0.56% PbO, < 0.05% FeO <sub>1.5</sub>
Massicot	PbO	1	< 0.18% CaO, < 0.11% FeO <sub>1.5</sub>

All concentrations are in mol.% cations

\*Within the uncertainty level

$$x(\text{FeO}_{1.5})^{\text{corr}} = x(\text{FeO}_{1.5}) + x(\text{CaO}) \cdot x(\text{FeO}_{1.5}) \cdot (0.0208 + 0.0119 \cdot (x(\text{FeO}_{1.5}) - x(\text{CaO}))) \quad (\text{Eq 2})$$

$$x(\text{CaO})^{\text{corr}} = 1 - x(\text{PbO})^{\text{corr}} - x(\text{FeO}_{1.5})^{\text{corr}} \quad (\text{Eq 3})$$

After correction, the compositions of secondary standards correspond to the stoichiometry within 0.1 mol.% standard deviation. The overall accuracy of reported compositions are believed to be within 1 mol.%, which includes all possible sources of errors (such as absence of secondary standards at intermediate Pb:Fe ratios, temperature uncertainty, difficulties in quenching, etc.).

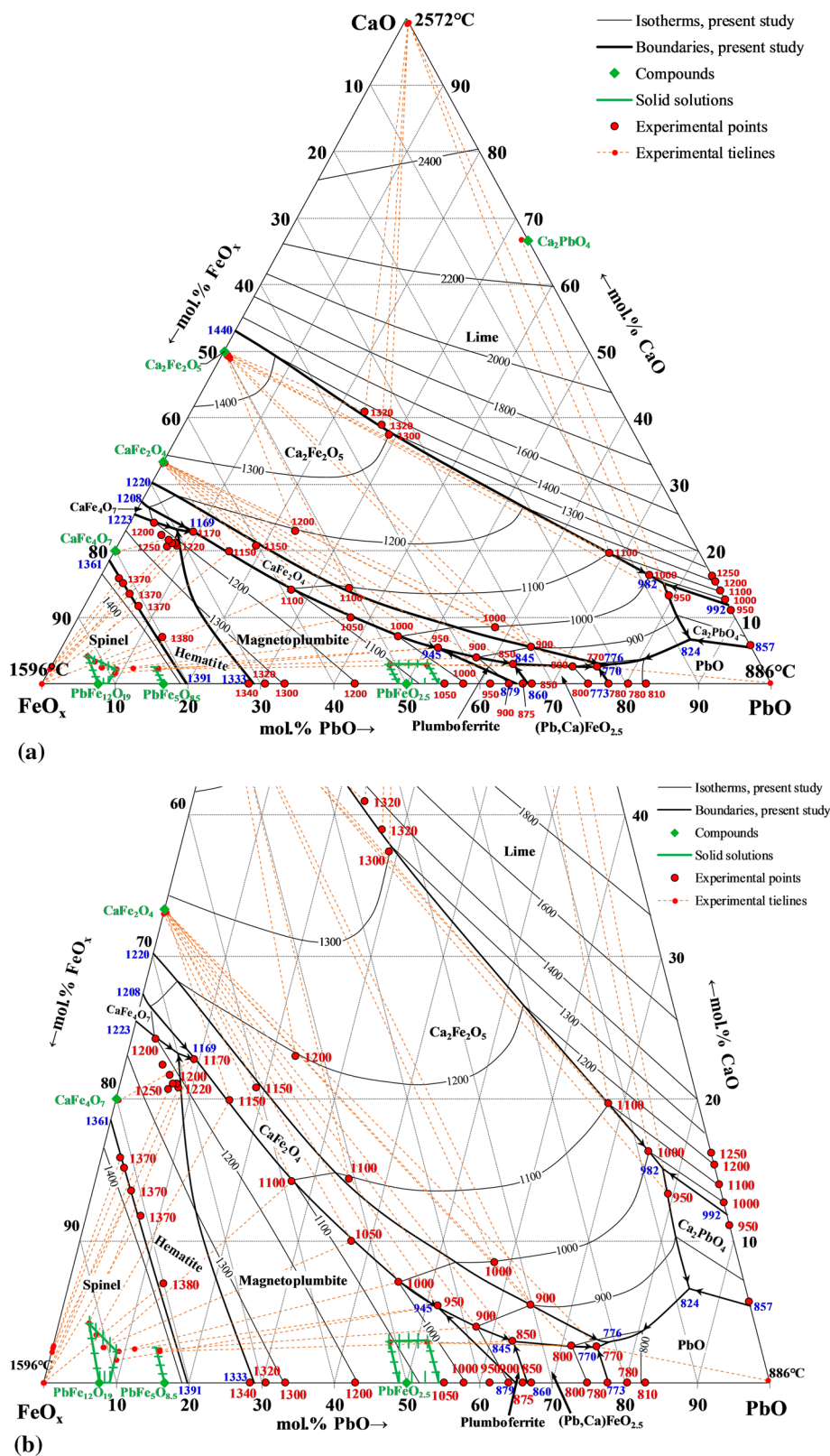
Only concentrations of metal cations were measured with EPMA. The ratios of the different oxidation states of iron cations were not measured in the present study, and the iron oxide concentrations were recalculated to FeO<sub>1.5</sub> for presentation purposes. According to the FactSage predictions,<sup>[13–16]</sup> the ferrous iron oxide (FeO) concentration in slags is very low (< 1 mol.%) for most of the range of conditions investigated.

The ability to produce samples containing the primary phase solids and glassy or amorphous phase on quenching depends on the composition of the slag and the

equilibration temperature. The most significant quenching difficulties were observed for the high-calcium slags in the lime primary phase field and high-iron slags in the spinel and hematite primary phase fields, where the areas of glassy homogeneous slag phase were limited to locations at the surfaces, directly contacting the quenching medium, the upper limit of temperatures therefore could not exceed 1593 K (1320 °C) for the lime and 1653 K (1380 °C) for the spinel and hematite primary phase fields. Another difficulty was fast PbO vaporization at such conditions, so that the equilibration times had to be limited to 15 min. The approach used to obtain accurate, repeatable, and objective measurements by the EPMA-line analysis was similar to the one described by Nikolic et al.,<sup>[21]</sup> in which the average composition of the liquid phase is calculated from 20 points measured in a well-quenched area within 15 microns from the surface, with the allowed limit of standard deviation < 1 wt.%. In cases of difficult quenching, the experiments were repeated many times until an area of appropriate well-quenched microstructure was found.

The absence of evaporation loss of the Pb species during EPMA measurement of a single point up to 1 min was confirmed in the present study. The accuracy of the EPMA

**Fig. 2** Liquidus surface of the PbO–“FeO<sub>1.5</sub>”–CaO system in air,  $p(\text{O}_2) = 0.21$  atm. Isotherms and boundary lines are drawn according to experimental results (where available) or estimated using FactSage database (at high temperatures) are in °C. (a) complete diagram; (b) enlarged part for  $x(\text{CaO}) < 42$  mol.%. PbO–“FeO<sub>1.5</sub>” binary is based on Ref 23; PbO–CaO results will be published elsewhere<sup>[20]</sup>



measurements was estimated to be within 1 wt.%, and the typical detection limit of minor components was estimated to be about 0.01 wt.%.<sup>[11]</sup> The major uncertainty sources of

the results include: deviation from targeted temperature and  $p(\text{O}_2)$ ; incomplete achievement of equilibrium, crystallization on quenching; sample contamination due to

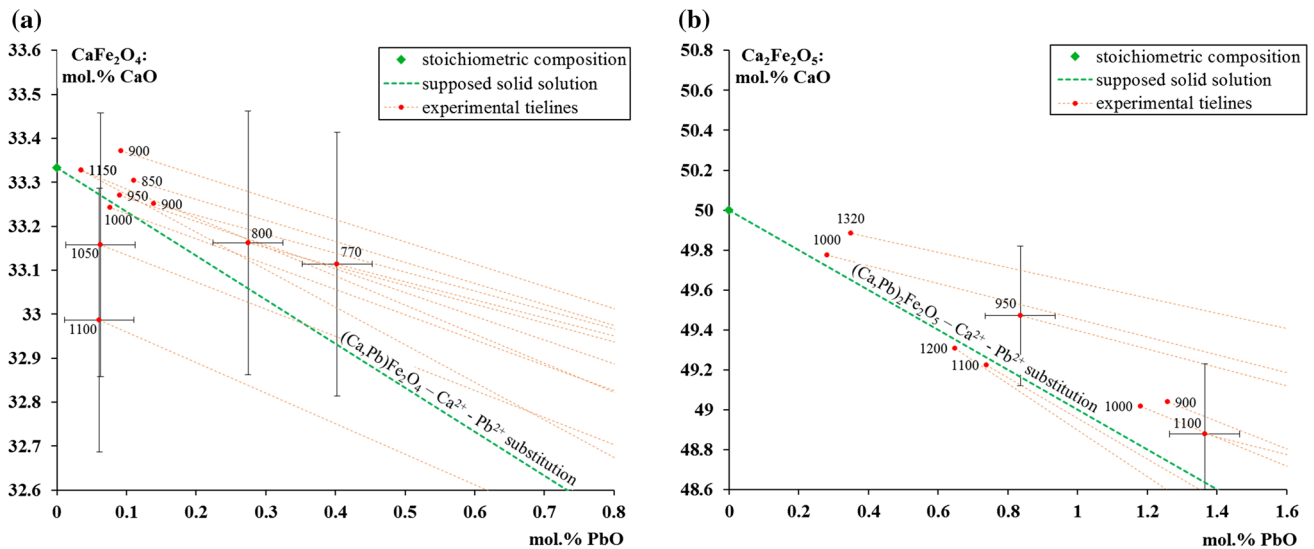
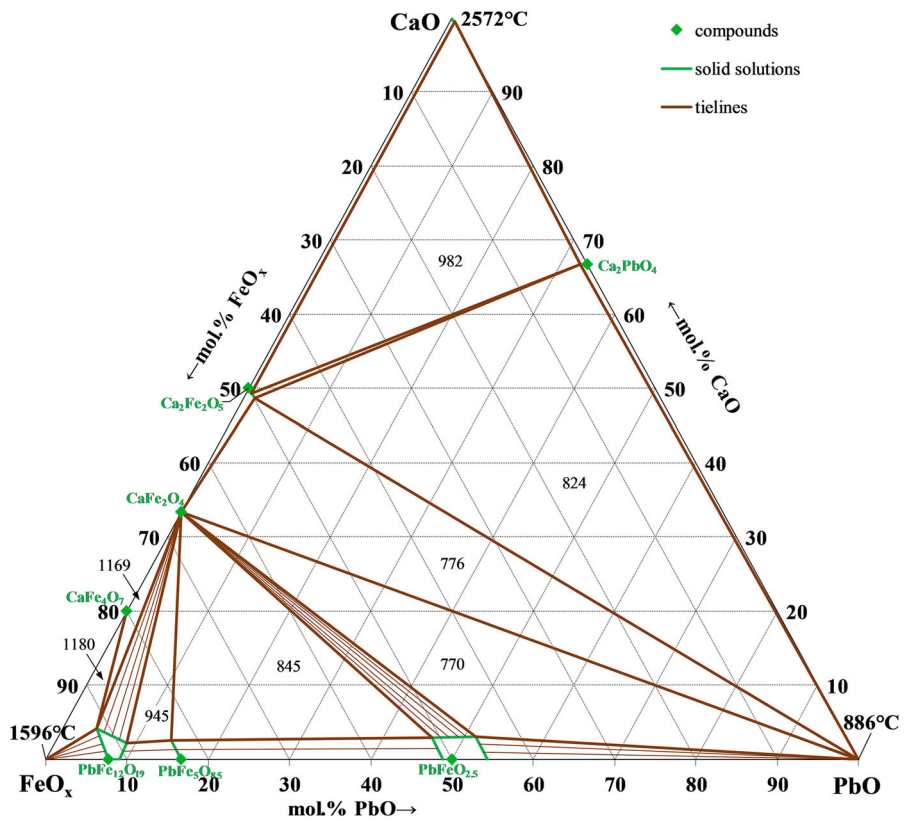


**Fig. 3** Compositions of  $\text{CaFe}_2\text{O}_4$  (a) and  $\text{Ca}_2\text{Fe}_2\text{O}_5$  (b) crystals in equilibrium with slags of the  $\text{PbO}$ -“ $\text{FeO}_x$ ”- $\text{CaO}$  system and air. Labels indicate the experimental temperatures ( $^\circ\text{C}$ )

**Fig. 4** Solidus surface of the  $\text{PbO}$ - $\text{CaO}$ -“ $\text{FeO}_{1.5}$ ” system in air,  $p(\text{O}_2) = 0.21 \text{ atm}$ . Temperatures ( $^\circ\text{C}$ ) and lines are presented according to experimental results (where available) or estimated using FactSage database



initial reagent impurities; surface roughness; EPMA standard analysis uncertainties; electron beam stability; EPMA ZAF correction uncertainties. Special attention was given in this study to continuously analyze and minimize all potential sources of uncertainties.

**2.2 Confirmation of Achievement of Equilibrium**

To ensure the achievement of equilibrium in the samples, the four-point test approach<sup>[17, 22]</sup> was used including: (1) variation of equilibration time; (2) assessment of the compositional homogeneity of phases by EPMA; (3)



approaching the final equilibrium point from different starting conditions; and, importantly, (4) consideration of reactions specific to this system that may affect the achievement of equilibrium or reduce the accuracy. Several dedicated series of experiments were carried out for these purposes, resulted in the experimental design features described below.

Calcium ferrite master-slag (70 mol.% “FeO<sub>1.5</sub>”, melting at ~ 1483 K (1210 °C)) was used to reduce the fraction of high-melting point calcium and iron oxides and remove most CO<sub>2</sub> from the initial mixture. This allowed to use lower premelting temperatures and consequently reduce Pb/PbO vaporization during the initial heating stage, suppress foaming of the slag, and reduce required equilibration time of the samples. Consequently, all initial mixtures were prepared from (Pb<sub>3</sub>O<sub>4</sub> + Fe<sub>2</sub>O<sub>3</sub> + master-slag) or (Pb<sub>3</sub>O<sub>4</sub> + CaCO<sub>3</sub> + master-slag) powders. The Pb<sub>3</sub>O<sub>4</sub> powder, prepared from PbO heated in air at 723 K (450 °C) for 24 h, was used instead of PbO to protect Pt and Au substrates from alloy formation with Pb metal and destruction that could take place due to local reducing conditions.

### 3 Results and Discussion

Examples of micrographs of quenched PbO-“FeO<sub>1.5</sub>”-CaO samples are given in Fig. 1(a-g). The results of all experiments with compositions of phases measured in this study are reported in Table 1. All solid phases observed in the system are summarized in Table 2.

No phases other than predicted by FactSage database<sup>[13–16]</sup> were discovered. Present experimental results were used to construct liquidus diagram presented in Fig. 2. There is a trough of relatively low liquidus temperatures along the magnetoplumbite-CaFe<sub>2</sub>O<sub>4</sub> boundary, separating the high-Ca and high-Fe parts of the diagram where the liquidus temperatures are much higher.

#### 3.1 Solid Solution Ranges in the PbO-“FeO<sub>1.5</sub>”-CaO System in Air

The ranges of compositions of the observed solid oxide phases in the PbO-“FeO<sub>1.5</sub>”-CaO system in air are listed in Table 2. Several compounds appear to have a range of solid solutions in this system: magnetoplumbite (Pb<sub>1-x</sub>Ca<sub>x</sub>)O·(12-y)FeO<sub>1.5</sub>; plumboferrite (Pb<sub>1-x</sub>Ca<sub>x</sub>)O·5FeO<sub>1.5</sub>; 1:1 lead ferrite (Pb<sub>1-x</sub>Ca<sub>x</sub>)O·yFeO<sub>1.5</sub>; “Ca<sub>2</sub>Fe<sub>2</sub>O<sub>5</sub>” (brownmillerite) (Ca<sub>1-x</sub>Pb<sub>x</sub>)O·FeO<sub>2.5</sub>. The ranges of solutions of the magnetoplumbite, plumboferrite and 1:1 lead ferrite are indicated in Fig. 2 with green crossed lines. Analysis of compositions of magnetoplumbite demonstrates that there is a systematic deficiency of Fe in the

compound compared to the ideal chemical formula (Pb,Ca)Fe<sub>12</sub>O<sub>19</sub>. Magnetoplumbite and plumboferrite are treated as separate solid solutions according to the present experimental results and previous study,<sup>[23]</sup> although future study may be needed to determine exact ranges of their compositions over wider range of conditions. Two points for 1:1 lead ferrite show significant variation of the Pb:Fe ratio (consistent with the earlier studies<sup>[23–26]</sup>), while the maximum CaO concentration (limited by the boundary with CaFe<sub>2</sub>O<sub>4</sub>) stays approximately the same.

Zoomed compositions and tielines for the CaFe<sub>2</sub>O<sub>4</sub> and Ca<sub>2</sub>Fe<sub>2</sub>O<sub>5</sub> compounds are shown in Fig. 3(a and b). Green dashed lines in Fig. 3 represent compositions of (Ca,Pb)Fe<sub>2</sub>O<sub>4</sub> and (Ca,Pb)<sub>2</sub>Fe<sub>2</sub>O<sub>5</sub>, where Ca is substituted with Pb in the crystal structure. The differences between these lines and the actual measurements are within the experimental uncertainties. For CaFe<sub>2</sub>O<sub>4</sub> (Fig. 3a), two low-temperature points, at 770 and 800 °C (1043 and 1073 K) represent more significant PbO solubility (0.3–0.4 mol.%) than the rest (< 0.15 mol.%). For Ca<sub>2</sub>Fe<sub>2</sub>O<sub>5</sub> (Fig. 3b), the accuracy of its composition measurement was hindered by its tendency to form very small crystals, particularly at low temperatures.

Calcium plumbate Ca<sub>2</sub>PbO<sub>4</sub> was found to dissolve 0.9 mol.% “FeO<sub>1.5</sub>” (single experiment); lime CaO—up to 0.34 mol.% “FeO<sub>1.5</sub>” and 0.56 mol.% PbO solubility; CaFe<sub>2</sub>O<sub>4</sub> and CaFe<sub>4</sub>O<sub>7</sub> both have up to 0.4 mol.% PbO solubility.

The solidus surface of the PbO-CaO-“FeO<sub>1.5</sub>” system in air is presented in Fig. 4. The invariant reaction temperatures (within possible 10 K uncertainty) are given according to present experimental results (if available) or estimated using preliminary FactSage thermodynamic database (for binary systems and at high temperatures).

### 4 Conclusions

New phase equilibria information in the PbO-“FeO<sub>1.5</sub>”-CaO system in air has been obtained. The range of temperatures investigated is 1043–1673 K (770–1380 °C), and included the equilibria of slag with one or two crystalline phases: hematite Fe<sub>2</sub>O<sub>3</sub>; spinel (Fe,Ca)Fe<sub>2</sub>O<sub>4</sub>; calcium ferrites CaFe<sub>4</sub>O<sub>7</sub>, CaFe<sub>2</sub>O<sub>4</sub>, Ca<sub>2</sub>Fe<sub>2</sub>O<sub>5</sub>; lead ferrites (magnetoplumbite (Pb,Ca)O·12FeO<sub>1.5</sub>, plumboferrite (Pb,Ca)O·(5 + x)FeO<sub>1.5</sub>, 1:1 lead ferrite (Pb,Ca)O·(1 ± x)FeO<sub>1.5</sub>); lead oxide PbO (massicot); calcium plumbate Ca<sub>2</sub>PbO<sub>4</sub>; lime CaO. This is the first systematic study of the Pb-Fe-Ca-O system in air, as a part of the multicomponent system Pb-Zn-Fe-Cu-Si-Ca-Al-Mg-O, essential for the lead smelting and recycling industries.

**Acknowledgments** The authors would like to thank Nyrstar (Australia), Outotec Pty Ltd (Australia), Aurubis AG (Germany), Umicore NV (Belgium), and Kazzinc Ltd, Glencore (Kazakhstan), and Australian Research Council Linkage Project LP150100783 for their financial support for this research. The authors are grateful to Prof. Peter C. Hayes (UQ) for valuable comments and suggestions, to Ms. Suping Huang for assistance with conducting experiments, and to the staff of the University of Queensland Centre for Microanalysis and Microscopy (CMM) for their support in maintenance and operation of scanning and electron microprobe facilities in the Centre.

## References

1. E. Jak, *Phase Equilibria to Characterise Lead/Zinc Smelting Slags and Sinters (PbO-ZnO-CaO-SiO<sub>2</sub>-Fe<sub>2</sub>O<sub>3</sub>-FeO)*, Ph.D Thesis (University of Queensland, 1995)
2. E. Jak, S.A. Decterov, P. Wu, P.C. Hayes, and A.D. Pelton, Thermodynamic Optimisation of the Systems PbO-SiO<sub>2</sub>, PbO-ZnO, ZnO-SiO<sub>2</sub> and PbO-ZnO-SiO<sub>2</sub>, *Metall. Mater. Trans. B*, 1997, **28B**, p 1011-1018
3. E. Jak, S.A. Decterov, P.C. Hayes, and A.D. Pelton, Thermodynamic Optimisation of the Systems CaO-Pb-O and PbO-CaO-SiO<sub>2</sub>, *Can. Metall. Q.*, 1998, **37**(1), p 41-47
4. E. Jak, N. Liu, and P.C. Hayes, Experimental Study of Phase Equilibria in the Systems PbO<sub>x</sub>-CaO and PbO<sub>x</sub>-CaO-SiO<sub>2</sub>, *Metall. Mater. Trans. B*, 1998, **29B**(3), p 541-553
5. E. Jak, B. Zhao, P.C. Hayes, S.A. Decterov, and A.D. Pelton, Coupled Experimental and Thermodynamic Modelling Studies of the System PbO-ZnO-FeO-Fe<sub>2</sub>O<sub>3</sub>-CaO-SiO<sub>2</sub>-Al<sub>2</sub>O<sub>3</sub> for Lead and Zinc Smelting, Zinc and Lead Processing, in ed. by J.E. Dutrizac, J.A. Gonzalez, G.L. Bolton, P. Hancock *1998 of Conference, Met. Soc. CIMM*, pp. 313–333
6. E. Jak, B. Zhao, N. Liu, and P.C. Hayes, Experimental Study of Phase Equilibria in the System PbO-ZnO-SiO<sub>2</sub>, *Metall. Mater. Trans. B*, 1999, **30B**(1), p 21-27
7. E. Jak and P.C. Hayes, Experimental Study of Phase Equilibria in the PbO-ZnO-Fe<sub>2</sub>O<sub>3</sub>-CaO-SiO<sub>2</sub> System in Air for High Lead Smelting Slags (CaO/SiO<sub>2</sub> = 0.35 and PbO/(CaO + SiO<sub>2</sub>) = 5.0 by Weight), *Metall. Mater. Trans. B*, 2002, **33B**(6), p 817-825
8. E. Jak and P.C. Hayes, Experimental Liquidus in the PbO-ZnO-Fe<sub>2</sub>O<sub>3</sub>-(CaO + SiO<sub>2</sub>) System in Air, with CaO/SiO<sub>2</sub> = 0.35 and PbO/(CaO + SiO<sub>2</sub>) = 3.2, *Metall. Mater. Trans. B*, 2002, **33B**(6), p 851-863
9. E. Jak and P.C. Hayes, The Effect of the CaO/SiO<sub>2</sub> Ratio on the Phase Equilibria in the ZnO-Fe<sub>2</sub>O<sub>3</sub>-(PbO + CaO + SiO<sub>2</sub>) System in Air: CaO/SiO<sub>2</sub> = 0.1, PbO/(CaO + SiO<sub>2</sub>) = 6.2, and CaO/SiO<sub>2</sub> = 0.6, PbO/(CaO + SiO<sub>2</sub>) = 4.3, *Metall. Mater. Trans. B*, 2003, **34B**(4), p 369-382
10. E. Jak, B. Zhao, I. Harvey, and P.C. Hayes, Experimental Study of Phase Equilibria in the PbO-ZnO-Fe<sub>2</sub>O<sub>3</sub>-(CaO + SiO<sub>2</sub>) System in Air for the Lead and Zinc Blast Furnace Sinters (CaO/SiO<sub>2</sub> Weight Ratio of 0.933 and PbO/(CaO + SiO<sub>2</sub>) Ratios of 2.0 and 3.2), *Metall. Mater. Trans. B*, 2003, **34B**(4), p 383-397
11. E. Jak, P.C. Hayes, and H.-G. Lee, Improved Methodologies for the Determination of High Temperature Phase Equilibria, *Met. Mater.*, 1995, **1**(1), p 1-8
12. M. Kudo, E. Jak, P.C. Hayes, K. Yamaguchi, and Y. Takeda, Lead Solubility in FeO<sub>x</sub>-CaO-SiO<sub>2</sub> Slags at Iron Saturation, *Metall. Mater. Trans. B*, 2000, **31B**(1), p 15-24
13. E. Jak, S.A. Decterov, P.C. Hayes, and A.D. Pelton, Thermodynamic Modelling of the System PbO-ZnO-FeO-Fe<sub>2</sub>O<sub>3</sub>-CaO-SiO<sub>2</sub> for Zinc/Lead Smelting, in *Proceedings of the 5th International Conference on Molten Slags, Fluxes and Salts* Iron and Steel Society (AIME, Sydney, Australia, 1997), pp. 621–628
14. E. Jak, S.A. Decterov, B. Zhao, A.D. Pelton, and P.C. Hayes, Coupled Experimental and Thermodynamic Modelling Studies for Metallurgical Smelting and Coal Combustion Slag Systems, *Metall. Mater. Trans. B*, 2000, **31B**(4), p 621-630
15. S.A. Decterov, I.-H. Jung, E. Jak, Y.-B. Kang, P. Hayes, and A.D. Pelton, Thermodynamic Modeling of the Al<sub>2</sub>O<sub>3</sub>-CaO-CoO-CrO-Cr<sub>2</sub>O<sub>3</sub>-FeO-Fe<sub>2</sub>O<sub>3</sub>-MgO-MnO-NiO-SiO<sub>2</sub>-S System and Applications in Ferrous Process Metallurgy, in ed. by C. Pistorius *SAIMM Symposium Series S36 (VII International Conference on Molten Slags, Fluxes & Salts)* (The South African Institute of Mining and Metallurgy, Johannesburg, Republic of South Africa, 2004), pp. 839–850
16. FactSage, Ecole Polytechnique, Montréal, <http://www.factsage.com/>, 2008
17. E. Jak, *Integrated Experimental and Thermodynamic Modelling Research Methodology for Metallurgical Slags with Examples in the Copper Production Field 9th International Conference on Molten Slags, Fluxes and Salts (MOLTEN12), 2012 of Conference (Beijing, China)*, The Chinese Society for Metals, W077
18. K.T. Jacob, G. Rajitha, and G.M. Kale, Thermodynamic Properties of Pb<sub>2</sub>PtO<sub>4</sub> and PbPt<sub>2</sub>O<sub>4</sub> and Phase Equilibria in the System Pb-Pt-O, *J. Alloys Compd.*, 2009, **481**(1–2), p 228-232
19. H. Fukuyama, K. Shimizu, and K. Nagata, Determination of Gibbs Energies of Formation of the Ca-Pt-O Compounds from Electromotive Force Method Using CaF<sub>2</sub> as Solid Electrolyte, *High Temp. Mater. Process.*, 2004, **23**(5–6), p 335-341
20. M. Shevchenko and E. Jak, *Experimental Liquidus Study of the Binary PbO-CaO and Ternary PbO-CaO-SiO<sub>2</sub> Systems*, Personal communication, PYROSEARCH (The University of Queensland, 2018)
21. S. Nikolic, P.C. Hayes, and E. Jak, Experimental Techniques for Investigating Calcium Ferrite Slags at Metallic Copper Saturation and Application to the Systems “Cu<sub>2</sub>O”-Fe<sub>2</sub>O<sub>3</sub>” and “Cu<sub>2</sub>O”-CaO at Metallic Copper Saturation, *Metall. Mater. Trans. B*, 2009, **40B**(6), p 892-899
22. M. Shevchenko, T. Hidayat, P. Hayes, and E. Jak, Liquidus of “FeO”-SiO<sub>2</sub>-PbO Slags in Equilibrium with Air and with Metallic Lead, Molten 2016, in *10th International Conference on Molten Slags, Fluxes and Salts, 2016 of Conference* (Seattle, Washington, USA), pp. 1221–1228
23. M. Shevchenko and E. Jak, Experimental Phase Equilibria Studies of the Pb-Fe-O System in Air, Equilibrium with Metallic Lead and at Intermediate Oxygen Potentials, *Metall. Mater. Trans. B*, 2017, **48**, p 2970-2983
24. M. Shevchenko and E. Jak, Experimental Liquidus Studies of the Pb-Fe-Si-O System in Equilibrium with Metallic Pb, *Metall. Mater. Trans. B*, 2017, **49**(1), p 159-180
25. J. Hadermann, A.M. Abakumov, I.V. Nikolaev, E.V. Antipov, and G. Van Tendeloo, Local Structure of Perovskite-Based “Pb<sub>2</sub>Fe<sub>2</sub>O<sub>5</sub>”, *Solid State Sci.*, 2008, **10**(4), p 382-389
26. D. Batuk, J. Hadermann, A. Abakumov, T. Vranken, A. Hardy, M. Van Bael, and G. Van Tendeloo, Layered Perovskite-Like Pb<sub>2</sub>Fe<sub>2</sub>O<sub>5</sub> Structure as a Parent Matrix for the Nucleation and Growth of Crystallographic Shear Planes, *Inorg. Chem.*, 2011, **50**(11), p 4978-4986